

Probabilistic analyses of soil consolidation by prefabricated vertical drains for single-drain and multi-drain systems

Mohammad Wasiul Bari¹, Mohamed A. Shahin^{2,*}† and Abdul-Hamid Soubra³

¹*Department of Civil Engineering, Rajshahi University of Engineering and Technology, Rajshahi 6204, Bangladesh*

²*Department of Civil Engineering, Curtin University, Perth, Western Australia 6845, Australia*

³*Department of Civil Engineering, University of Nantes, Saint-Nazaire, France*

SUMMARY

Natural soils are one of the most inherently variables in the ground. Although the significance of inherent soil variability in relation to reliable predictions of consolidation rates of soil deposits has long been realized, there have been few studies that addressed the issue of soil variability for the problem of ground improvement by prefabricated vertical drains. Despite showing valuable insights into the impact of soil spatial variability on soil consolidation by prefabricated vertical drains, available stochastic works on this subject are based on a single-drain (or unit cell) analyses. However, how the idealized unit cell solution can be a supplement to the complex multi-drain systems for spatially variable soils has never been addressed in the literature. In this study, a rigorous stochastic finite elements modeling approach that allows the true nature of soil spatial variability to be considered in a reliable and quantifiable manner, both for the single-drain and multi-drain systems, is presented. The feasibility of performing an analysis based on the unit cell concept as compared with the multi-drain analysis is assessed in a probabilistic context. It is shown that with proper input statistics representative of a particular domain of interest, both the single-drain and multi-drain analyses yield almost identical results. Copyright © 2016 John Wiley & Sons, Ltd.

Received 11 June 2015; Revised 2 March 2016; Accepted 1 April 2016

KEY WORDS: soil consolidation; prefabricated vertical drains; ground improvement; soil spatial variability; finite elements; numerical modeling; probabilistic analyses

INTRODUCTION

The use of prefabricated vertical drains (PVDs) in combination with pre-loading is becoming one of the most commonly used methods for promoting radial drainage to accelerate the time rates of soil consolidation. Natural soils, however, are highly variable in the ground because of the uneven soil micro fabric, geological deposition, and stress history, and soil consolidation by PVDs is strongly dependent on spatially variable soil properties, most significantly is the coefficient of consolidation. The review of relevant literature has indicated that although the significance of inherent soil variability in relation to reliable predictions of soil consolidation rates has long been realized [1], only few studies (e.g., [2–5]) have investigated the problem of ground improvement by PVDs for spatially variable soils, using stochastic analyses. Despite showing valuable insights into the impact of soil spatial variability on soil consolidation, available stochastic studies for PVD-improved ground have been based on an idealized single-drain (or unit cell) system rather than the actual full multi-drain situation. A design procedure for PVD-ground improvement incorporating soil spatial variability for the single-drain concept was previously developed by Bari and Shahin [6], and in the

*Correspondence to: Mohamed A. Shahin, Department of Civil Engineering, Curtin University, Perth, Western Australia 6845, Australia.

†E-mail: m.shahin@curtin.edu.au

current study, the multi-drain system will be considered, and its results will be compared with those of the single-drain system. More importantly, a methodology will be developed for the unit cell analysis to achieve an equivalent solution to that of the multi-drain system with a much reduced computational cost.

Indeed, soil improvement via PVDs typically consists of hundreds of drains installed in the form of square or triangular patterns, with spacing varied between 1 and 3 m. This means that the consolidating area (including all the drains) can be significantly large and computationally too expensive for any numerical deterministic analysis. This computational cost becomes prohibitive when conducting a probabilistic analysis because each soil configuration requires a significant number of calls of the deterministic model in the order of several hundreds, when searching the first two statistical moments (i.e., mean and standard deviation) of a system response. The number of calls becomes even very large (about several thousands) when computing a small value of probability of occurrence of an undesirable event. In order to reduce the computational effort within the deterministic context, a full three-dimensional (3D) multi-drain system is usually simulated by considering a soil cylinder with a single central vertical drain so that the consolidation problem can be analyzed at the unit cell level. Each unit cell is assumed to be identical, having the same homogeneous soil, and thus the single-drain analysis is often sufficient to represent the overall soil consolidation behavior [7]. However, for spatially variable soils, the unit cell idealization used to represent the multi-drain system may not lead to identical solutions. Therefore, the aim of this paper is to investigate the conditions that need to be employed into the idealized unit cell analysis so as to establish stochastic equivalence between the unit cell and multi-drain analyses.

In order to treat soil spatial variability in most geotechnical engineering problems, stochastic computational schemes that combine the finite elements (FE) method and Monte Carlo technique are often used (e.g., [2, 6, 8, 9]). The same approach is adopted in the present study, which allows the soil spatial variability to be considered in a quantifiable manner, both for the single-drain and multi-drain analyses. The approach involves the development of advanced numerical models that merge the local average subdivision (LAS) technique [10] of the random field theory [11] and the FE method into a Monte Carlo framework. For the case of PVDs, the overall consolidation is governed by the horizontal radial* flow of water rather than the vertical flow because the drainage length in the horizontal direction is usually much less than that of the vertical direction and the horizontal permeability is often much higher than the vertical one [12]. Under such reasoning, soil consolidation by PVDs in the current study is considered by 2D radial drainage problem (for both cases of idealized unit cell and multi-drain systems). The probabilistic results (i.e., the mean and standard deviation of the degree of consolidation and probability of achieving a target degree of consolidation) as obtained from both the idealized unit cell model and multi-drain model are presented for different conditions imposed on the unit cell case to determine the necessary conditions leading to equivalence between the two probabilistic analyses. In the sections that follow, the stochastic finite elements Monte Carlo (FEMC) approach is described in some detail followed by detailed demonstration and discussion of the obtained results.

STOCHASTIC FINITE ELEMENTS MONTE CARLO APPROACH

As indicated earlier, the equivalence between the single-drain and multi-drain systems is examined by employing a stochastic FEMC approach, which has the following steps:

1. Create a virtual soil profile that represents a realization of designated spatially varying soil properties, allowing the correlation structure (expressed by the autocorrelation function) of the soil properties to be realistically simulated.
2. Incorporate the generated realization of soil profile into FE modeling of soil consolidation by PVDs.
3. Repeat Steps 1 and 2 several times using the Monte Carlo technique. Each time, a new realization of virtual soil profile (Step 1) is created and implemented into a subsequent FE analysis (Step 2).

*Radial herein means that the flow is occurring towards the PVD and not necessary being in straight lines.

At the end, a series of values of the degree of consolidation is obtained from which the following two items can be estimated: (i) the first two statistical moments of the degree of consolidation and (ii) the probability of achieving a target degree of consolidation.

The aforementioned steps, as well as the numerical procedures, are described in some detail in the succeeding discussion.

Simulation of virtual soil profiles

In order to warrant the true influence of soil spatial variability for the problem at hand, virtual soil profiles that allow the rational distributions of designated spatially variable soil properties across the soil mass need to be generated (based on a predefined probability density function, PDF, and a prescribed spatial correlation function), which can then be implemented into the FE modeling. Prior to proceeding with this step, it is necessary to identify the soil properties that have the most significant impact on soil consolidation by PVDs so that they can be treated as random fields when creating the virtual soil profiles. The spatial variability of several soil properties can affect soil consolidation by PVDs. However, as far as the 2D horizontal drainage is concerned, which is the case considered in the current study, the coefficient of horizontal consolidation, c_h , is the most significant random soil property affecting the behavior of soil consolidation by PVDs, as indicated by many researchers (e.g., [4, 5]). Accordingly, in the current study, c_h is considered to be spatially variable, whereas the other soil properties are held constant and treated deterministically so as to reduce the superfluous complexity of the problem.

The spatial variability of c_h is assumed to be characterized by lognormal distribution because observation obtained from field data reported by Chang [13] suggested that the variation of c_h can be adequately modeled by a lognormal distribution. Based on the random field theory, a spatially variable soil property with lognormal distribution and predefined autocorrelation function can be characterized by (i) the soil property mean value, μ , the variance, σ^2 (which can also be represented by the standard deviation, σ , or coefficient of variation, v , where $v = \sigma/\mu$); and (ii) the correlation length, θ (also known as scale of fluctuation), which appears within the predefined autocorrelation function. The value of θ describes the limits of spatial continuity and can simply be defined as the distance over which a soil property shows considerable correlation between two spatial points. Therefore, a large value of θ indicates strong correlation (i.e., uniform soil property field), whereas a small value of θ implies weak correlation (i.e., erratic soil property field). In this paper, the horizontal coefficient of consolidation c_h is assumed to be spatially variable, in both directions of the (x - y) horizontal plane and also be statistically isotropic, that is, the correlation lengths in the x and y coordinates are assumed to be the same (i.e., $\theta_{\ln c_h(x)} = \theta_{\ln c_h(y)} = \theta_{\ln c_h}$). The reason for assuming isotropic c_h is that the correlation structure is more related to the formation process (i.e., layer deposition) in the horizontal (x - y) plane. The correlation coefficient between c_h measured at a point A (x_1, y_1) and a second point B (x_2, y_2) is specified in this paper by an exponentially decaying spatial correlation function, $\rho(\tau)$, as follows [10]:

$$\rho(\tau) = \exp\left(-\frac{2\tau}{\theta_{\ln c_h}}\right) \quad (1)$$

where τ is the distance separating the two points A and B and $\theta_{\ln c_h}$ is the isotropic correlation length. It can be seen from Equation (1) that the spatial correlation length is estimated with respect to the underlying normally distributed field, that is, $\ln(c_h)$.

In the current study, the LAS method [10], which is a fast and largely accurate method of generating realizations of Gaussian random field, is used to produce 2D random fields of c_h for soil consolidation under horizontal drainage conditions. The concept of LAS approach was first extracted from the stochastic subdivision algorithm [14] and then incorporated the local averaging theory [15] into it. Because c_h is assumed to be 2D random field, a brief overview of the 2D implementation of LAS is presented herein. The 2D LAS method involves a several staged subdivision process in which a parent cell is divided into four (2×2) equal sized cells at each stage. The parent cells of the previous stage are used to obtain the best linear estimates of the mean of each new cell in such a way that the

upward averaging is preserved and they are properly correlated with each other. The linear estimation of the mean is accomplished by using the covariance between the local averages over each cell. At Stage 0, an initial network of low resolution field (parent cells for Stage 1) is generated directly using Cholesky decomposition. As shown in Figure 1, the parent cells from Stage 0 denoted as G_l^i (where, $l=1, 2, 3, \dots$) is subdivided into four equal sized cells (child cells) at Stage 1 and are then denoted as G_j^{i+1} , (where, $j=1, 2, 3, \dots$). Although each parent cell is eventually subdivided in the LAS process, subdivision of only G_5^i is shown in Figure 1 for simplicity.

Following the aforementioned process, correlated local averages of standard normal random field $G(x)$ are first generated with zero mean, unit variance, and spatial correlation function. The required lognormally distributed random field of c_h defined by μ_{c_h} and σ_{c_h} is then obtained using the following transformation function [10]:

$$c_{h_i} = \exp\{\mu_{\ln c_h} + \sigma_{\ln c_h} G(x_i)\} \tag{2}$$

where x_i and c_{h_i} are, respectively, the vectors containing the coordinates of the centers of the soil elements and the soil property values assigned to those elements and $\mu_{\ln c_h}$ and $\sigma_{\ln c_h}$ are, respectively, the mean and standard deviation of the underlying normally distributed c_h , that is, $\ln(c_h)$. The LAS algorithm generates realizations of c_h in the form of a grid of cells that are assigned locally averaged values of c_h different from one another across the soil mass, by taking full account of the FEs size in the local averaging process, albeit remained constant within each element of the discretised soil domain.

Finite elements modeling incorporating soil spatial variability

The 2D spatial variation of c_h simulated in the previous step is mapped onto the refined FE mesh, and the consolidation analysis is followed. A modified version of the FE computational scheme ‘Program 8.6’ as presented in the book by Smith and Griffiths [16] is used in this study to carry out all the numerical modeling analyses. The simplest form of the governing consolidation equations with the assumption that the laminar flow through the saturated soil (Darcy’s law) is valid can be expressed by Equation (3), which forms the basis of this program allowing multidimensional consolidation analysis over a general FE mesh, and is expressed as follows:

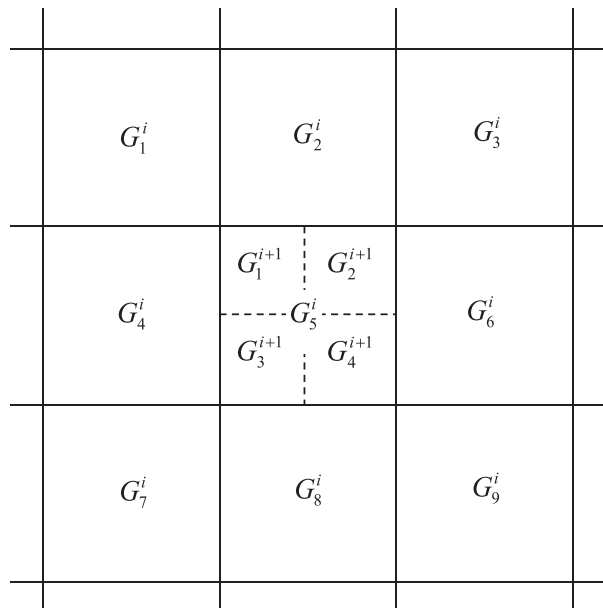


Figure 1. Local average subdivision in two dimensions (after [29]).

$$c_x \frac{\partial^2 u_w}{\partial x^2} + c_y \frac{\partial^2 u_w}{\partial y^2} + c_z \frac{\partial^2 u_w}{\partial z^2} = \frac{\partial u_w}{\partial t} \quad (3)$$

It can be noticed in Equation (3) that there is only a single dependent variable (i.e., pore pressure) and the analysis is thus ‘uncoupled’ (i.e., no displacement degrees of freedom). Originally, ‘Program 8.6’ was for general 2D or 3D analyses of uncoupled consolidation equation using an implicit time integration with the ‘theta’ method, and interested readers are referred to Smith and Griffiths [16] for the description of such method. The authors have modified the source code of ‘Program 8.6’ to allow repetitive stochastic Monte Carlo analyses. Although the modified version of ‘Program 8.6’ can also be used for 3D analysis, 2D FEMC analyses are conducted in the current study as the drainage of water is assumed to take place in the horizontal direction only, as discussed previously.

The multi-drain influence area is assumed to be equal to a square of 3.8×3.8 m containing 16 drains (4×4), which is equivalent to the sum of each influence area (0.95×0.95 m) of all individual drains (Figure 2). The spacing, S , between the drains is assumed to be equal to 0.95 m (Figure 2a). On the other hand, the drain spacing, S , in the multi-drain analysis represents the side length, S , of the square influence area in the single-drain ‘unit cell’ analysis (Figure 2b). It should be noted that the band-shaped PVD is transformed into a square shaped of a side length, $S_w = \frac{\pi r_w}{2}$ (where the equivalent radius of the drain, r_w , is assumed equal to 0.032 m). This is because the LAS method requires square (or rectangular) elements to be able to accurately compute locally averaged values of c_h for each element across the grid. Notice also that, for simplicity, the well resistance, which may affect the rate of consolidation, is not considered in the current study. This is because the discharge capacities of most PVDs available in the market are relatively high; hence, the impact of well resistance can be ignored in most practical cases, as suggested by many researchers (e.g., [17]).

Generally speaking, the more FEs in the mesh used to discretize the domain of the problem, the greater the accuracy of the FE solution. However, a trade-off between accuracy and run-time efficiency is necessary. Previous literature reported some recommendations regarding the optimum ratio of the correlation length to the size of the FEs. For example, Ching and Phoon [18] stated that this ratio should be ≥ 20 , whereas Harada and Shinozuka [19] pointed out that it should be ≥ 2 . In the current study, a sensitivity analysis on two different FE meshes with element sizes of 0.05 and 0.025 m is considered, for the purpose of obtaining the optimum mesh discretization. For a certain correlation length, two random fields of two selected meshes are generated using the same seed

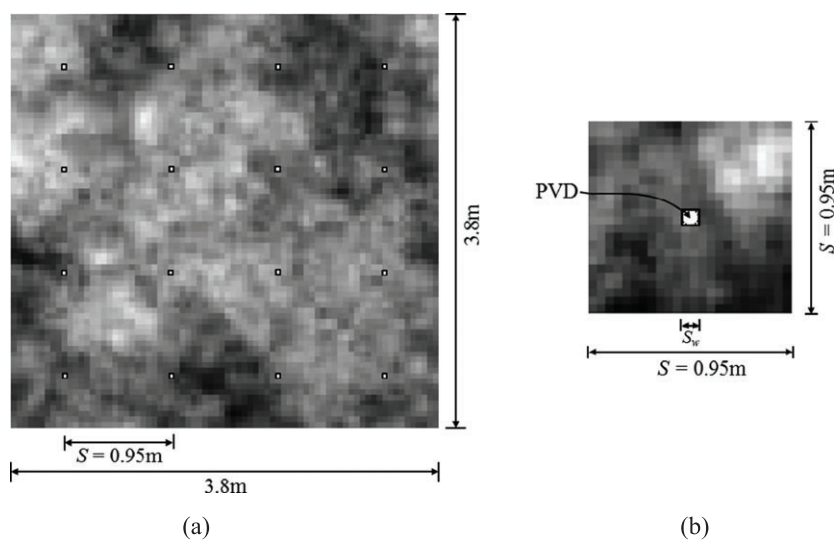


Figure 2. Realizations of prefabricated vertical drain (PVD)-improved ground: (a) 16 drains in a square grid pattern and (b) single-drain in a square geometry.

value, and FE analyses are conducted. The results obtained from the two meshes are then compared to see if they are identical; otherwise, finer meshes are generated, and the previous process is repeated. Several different random seeds and correlation lengths are tested for the highest coefficient of variation of c_h considered in this study. It is found that 0.05 and 0.025 m meshes gave nearly identical solutions, as long as the ratio of the correlation length to FE size ≥ 2 , which complies with the recommendation given by Harada and Shinozuka [19] albeit disagrees with the ratio recommended by Ching and Phoon [18]. This is because the ratio of 20 recommended by Ching and Phoon (2013) was for a shear strength problem, which is different from the consolidation problem as the spatial average shear strength is computed along the most critical slip surface rather than over the entire domain that is usually used for the consolidation problems. Based on the aforementioned discussion, a mesh with elements size of 0.05×0.05 m, which is more than two times smaller than the minimum correlation length, is adopted in the current study.

The initial condition for the uncoupled consolidation approach (i.e., no displacement degrees of freedom and only pore pressure degrees of freedom) is such that the excess pore pressure at all nodes (except at the nodes of the drain boundary) is set to be equal to 100 kPa, while the excess pore pressure at each node of the drain boundary is set to be zero. After generating a given realization and subsequent FE consolidation analysis of that realization, the corresponding degree of consolidation, $U(t)$, at any consolidation time, t , is calculated based on the excess pore pressure concept with the help of the following expression:

$$U(t) = 1 - \frac{\bar{u}(t)}{u_0} \quad (4)$$

where u_0 is the initial uniform excess pore water pressure and $\bar{u}(t)$ is the average excess pore water pressure. It has to be emphasized that the average excess pore pressure $\bar{u}(t)$ at any time during the consolidation process is calculated by numerically integrating the excess pore water pressures across the entire area of the mesh and dividing it by the total mesh area.

Repetition of process based on Monte Carlo technique

By applying the Monte Carlo technique (on either the unit cell system or the multi-drain approach), the process of generating a realization of c_h and the subsequent FE consolidation analysis are repeated numerous times until convergence of the estimated statistical outputs (i.e., mean μ_U and standard deviation σ_U of $U(t)$ and probability P of achieving a target value of $U(t)$) is obtained. Convergence is deemed to be achieved if there is stabilization in the first two statistical moments (mean and standard deviation) as the number of simulations increases. It should be emphasized that the three quantities $\mu_U(t)$, $\sigma_U(t)$, and $P(t)$ are all functions of the time t ; however, the symbol t is omitted later for simplicity. A total number of simulations of 2000 are used for all probabilistic computations throughout the paper. This number is much beyond the one required to achieve convergence for the first two statistical moments of the degree of consolidation (i.e., mean, μ_U , and standard deviation, σ_U). It can be seen from Figure 3a and b that 400 simulations are sufficient to achieve the required convergence (as far as the convergence are concerned, the single-drain analysis with coefficient of variation of $c_h = 100\%$ and $\theta_{inc_h} = 4.0$ m shows the worst result). Notice however that (Figure 3c) the number of 2000 simulations was necessary to arrive to an acceptable maximal value (of about 5%) of the coefficient of variation of P at its value equal to 90%. It should be noted that the probabilistic analysis of a single configuration (corresponding to prescribed μ_{c_h} , σ_{c_h} , and θ_{inc_h}) with 2000 Monte Carlo simulations typically takes around 1 h for the single-drain analysis and it takes about 30 h for the multi-drain analysis on an Intel core i5 CPU at 3.4 GHz computer. Notice also that although each simulation of the Monte Carlo process involves the same μ_{c_h} , σ_{c_h} , and θ_{inc_h} , the spatial distribution of c_h varies from one simulation to the next while preserving the correlation structure of the random field.

The obtained $U(t)$ from the suite of 2000 realizations of the Monte Carlo process are collated, and μ_U and σ_U of the degree of consolidation over the 2000 simulations are estimated as a function of t using the method of moments, while the probability of achieving a target degree of consolidation, U_s (i.e., $P[U \geq U_s]$), at specified consolidation time, t_s , is simply estimated by counting the number of simulations in which $U \geq U_s$ (i.e., $N_{U \geq U_s}$) and dividing it by the total number of simulations, N_{sim} . As

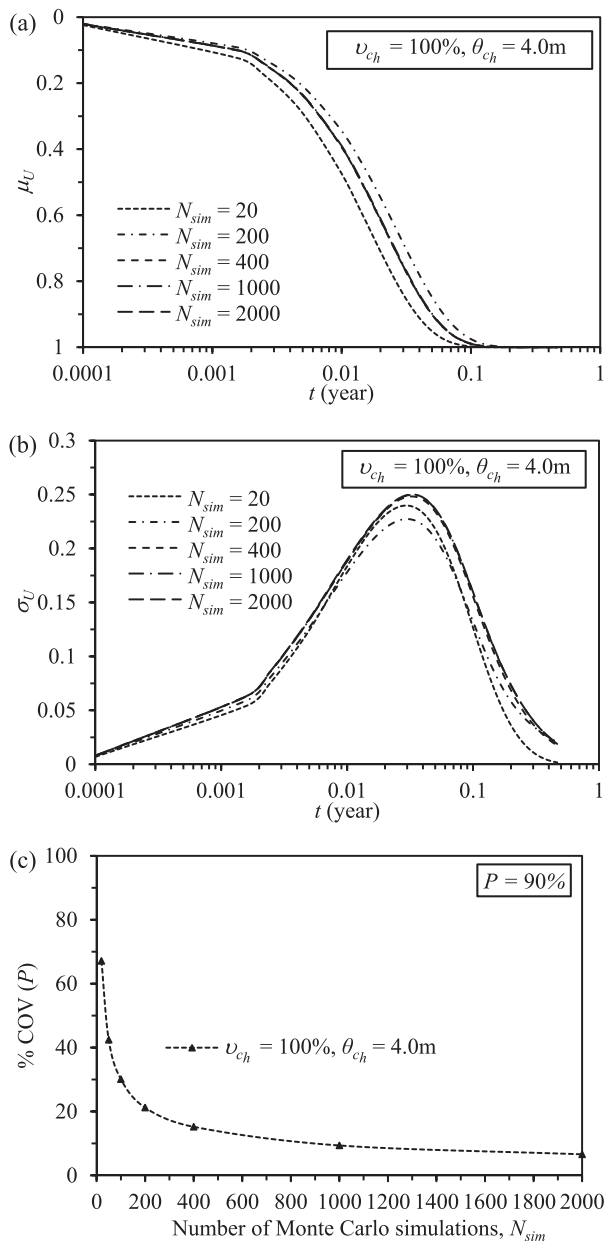


Figure 3. Effect of N_{sim} on (a) μ_U , (b) σ_U , and (c) $COV(P)$ at $P=90\%$ for $v_{ch} = 100\%$ and $\theta_{inc_h} = 4.0\text{ m}$.

90% consolidation, U_{90} , is usually acceptable for the purpose of design of most soil improvement projects [20], U_{90} is thus assumed to be the target degree of consolidation (i.e., $U_s = 90\%$) in this study. On the other hand, the probability of achieving 90% target degree of consolidation, $P [U \geq U_{90}]$, is estimated from the sampled values of U and expressed as a function of t .

PARAMETRIC STUDIES

Following the stochastic FEMC procedure set out in the previous section, parametric studies are performed to investigate the equivalence between the single-drain and multi-drain analyses in terms of μ_U , σ_U , and $P[U \geq U_{90}]$ of the degree of consolidation. For this purpose, two groups of FEMC

analyses are performed. In the first group, the point mean and standard deviation and the correlation length are assumed to be the same for both the single-drain and multi-drain cases, whereas in the second group, the associated point statistics of each soil domain are derived in such a way that their underlying local average statistics remain the same.

Results considering same point statistics for both single-drain and multi-drain cases

The results obtained from the single-drain and multi-drain FEMC analyses employing the same point random field parameters are compared in this section for different combinations of σ_{c_h} and θ_{inc_h} , while μ_{c_h} is kept at a fixed value equal to 15 m²/year. It should be noted that σ_{c_h} is presented herein by a non-dimensional parameter called the coefficient of variation, v_{c_h} , where $v_{c_h} = \sigma_{c_h} / \mu_{c_h}$. The values of v_{c_h} and θ_{inc_h} used in the analyses are as follows:

- $v_{c_h} = 25, 50, \text{ and } 100$ (%); and
- $\theta_{inc_h} = 0.5, 1.0, 4.0, 16, \text{ and } 100$ (m)

The aforementioned selected range of v_{c_h} is typical to that reported in the literature (e.g., [21]). Unlike the coefficient of variation of soil properties, the correlation length (or θ_{inc_h}) is less well documented, particularly in the horizontal direction. However, Phoon and Kulhawy [22] reported suggested guidelines for the range of correlation length of soil properties based on a comprehensive review of various test measurements and found that the horizontal correlation length typically ranges between 3 and 80m, while the typical range of vertical correlation length is 0.8 to 6.2m, as observed in real soils [18]. On the other hand, Popescu *et al.* [23] reported that the correlation length is dependent on the sampling intervals but that closely spaced data are rarely available in the horizontal direction. Accordingly, a wide range of correlation length is selected in this study where its minimum and maximum values are specified to be equal to 0.5 and 100 m, respectively.

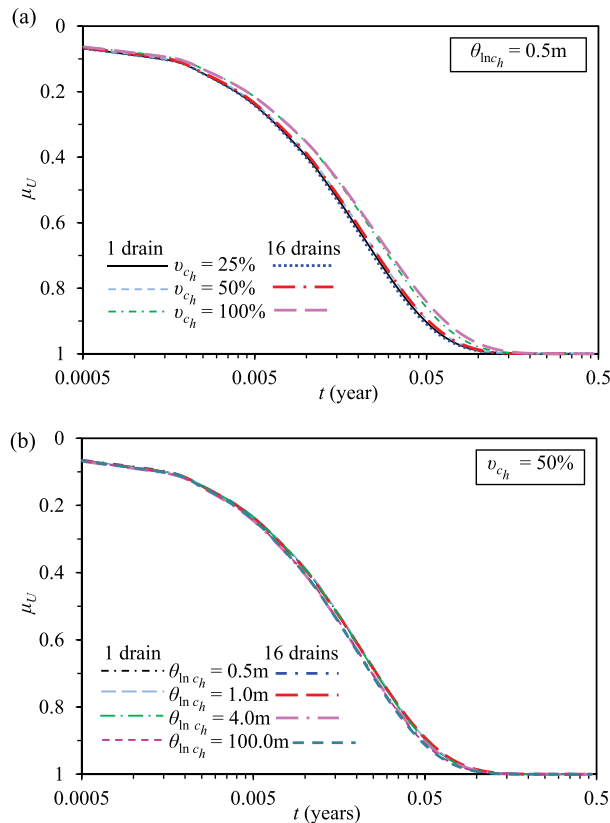


Figure 4. Comparison between μ_U computed from the same point statistics for (a) various v_{c_h} at $\theta_{inc_h} = 0.5$ m and (b) various θ_{inc_h} at $v_{c_h} = 50\%$.

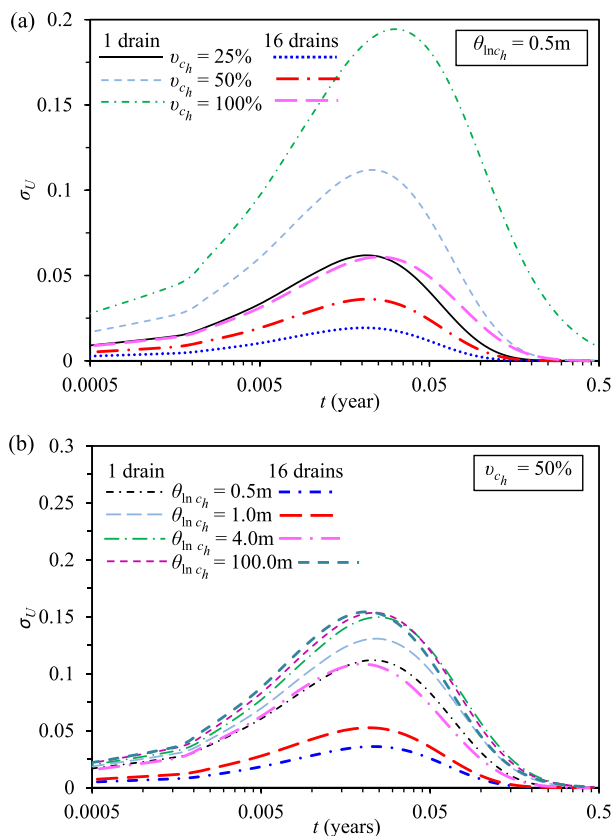


Figure 5. Comparison between σ_U computed from the same point statistics for (a) various v_{c_h} at $\theta_{inc_h} = 0.5$ m and (b) various θ_{inc_h} at $v_{c_h} = 50\%$.

The sensitivity of μ_U and σ_U on the statistically defined input data (i.e., v_{c_h} and θ_{inc_h}) is examined in Figures 4 and 5 in which μ_U and σ_U are expressed as functions of the consolidation time t . The comparison between μ_U derived from the single-drain and multi-drain FEMC simulations is examined in Figure 4. The effect of increasing v_{c_h} on μ_U at a fixed value of $\theta_{inc_h} = 0.5m$ is illustrated in Figure 4a, which indicates that μ_U obtained from the single-drain case agrees very well with that obtained from the multi-drain counterpart, for all cases of v_{c_h} . For both domains of analysis, μ_U decreases with the increase of v_{c_h} . On the other hand, Figure 4b shows the variation of μ_U as estimated by the single-drain and multi-drain FEMC analyses, for various values of θ_{inc_h} and at a fixed value of $v_{c_h} = 50\%$. In general, it can be observed that the results for various θ_{inc_h} are embodied into a single curve (Figure 4b), implying that the obtained results at different θ_{inc_h} are very close and cannot be distinguished. The virtually identical curves for all θ_{inc_h} demonstrate that μ_U obtained from the single-drain and multi-drain cases are almost identical.

The possible stochastic equivalence between the single-drain and multi-drain analyses is further examined via matching the estimated σ_U at different values of v_{c_h} and θ_{inc_h} , as shown in Figure 5. It can be seen that σ_U obtained from the single-drain case is significantly higher than that obtained from the multi-drain case and the difference in σ_U between the two solutions increases as v_{c_h} increases (Figure 5a). For $v_{c_h} = 100\%$, the difference in σ_U between the two solutions at time corresponding to the maximum value of σ_U is as high as 215%. This can be explained as follows: because the averaging domain is significantly smaller for the single-drain case compared with the multi-drain case, there is less variance reduction (for a certain θ , the variance reduction increases with the increase in the domain size and vice versa), resulting in higher σ_U in the single-drain case than the multi-drain solution. The influence of θ_{inc_h} on the compliance between the single-drain and multi-drain solutions in terms of σ_U at a fixed value of $v_{c_h} = 50\%$ is emphasized in Figure 5b. It can be seen that considerable differences in σ_U (as obtained from the two solutions) are found particularly when θ_{inc_h} is as low as 0.5m. The

difference in σ_U between the two solutions at time corresponding to the maximum value of σ_U is about 210% for $\theta_{\ln c_h} = 0.5$ m. On the other hand, little or no difference in σ_U is found for very high $\theta_{\ln c_h}$ (e.g., 100.0 m). This is because when $\theta_{\ln c_h} \gg D$ (where D is the size of the problem), the variance reduction factor $\gamma(D) \rightarrow 1.0$, implying no variance reduction (the details about $\gamma(D)$ will be explained later in the following section). It can also be seen from Figure 5 that the maximum σ_U occurs at an intermediate t , while σ_U is zero at $t=0$ and at large t . This can be explained by noting that $U(t)$ approaches 0 and 1 as t approaches 0 and ∞ , regardless of the variability of c_h .

From the aforementioned results, it is clear that by employing the same point statistics for both the single-drain and multi-drain cases, the stochastic response of soil consolidation by PVDs is different except for extremely large correlation length in comparison with the size of the problem domain. This means that the point statistics of soil property, which is representative of one domain, may not be considered as representative of another domain of different size unless the correlation length is very large in both domain sizes. Therefore, the logical question that should be asked is that how the spatially variable soil property statistics of one domain (e.g., multi-drain) can be used in another domain of different dimension (e.g., single drain) to achieve identical probabilistic consolidation solutions. This question can be answered by employing the concept of local averaging, which is discussed in the succeeding discussion.

Results considering same local average statistics for both single-drain and multi-drain cases

In the random field context, the input parameters in relation to the random soil properties (i.e., μ_{c_h} , σ_{c_h} , and $\theta_{\ln c_h}$ of c_h) are usually defined at the point level. Detailed description of the methods used for evaluating spatial variation of soil properties at the point level is beyond the scope of the present paper and can be found in many publications (e.g., [24, 25]). Although the random field is characterized by their point statistics, Vanmarcke [26] pointed out that it is not the point scale characteristics of random soil properties that govern the performance of geotechnical structures but rather the local average soil properties. Thereby, the stochastic equivalence between the idealized single-drain and multi-drain analyses may therefore be achieved if the local average statistics for both resolutions are the same. The suitability of using the concept of the local average statistics for problems involving large spatial mechanisms (e.g., bearing capacity, settlement of foundations, and slope stability) has been examined by many researchers (e.g., [27, 28]). However, for problems with preferential flow path (e.g., soil consolidation by PVDs), the local variability may be significant because some worse case combination of the random filed parameters may cause blockage to the flow because of lack of flow option in the system, particularly for one 1D and 2D geometries. Therefore, the effectiveness of the local average statistics to establish stochastic equivalence between the single-drain and multi-drain systems needs a thorough investigation, as follows.

It should be noted that the local average statistics associated with the input point statistics depend on several factors, namely [29], (i) the size of the averaging domain, D ; (ii) the correlation function, ρ ; and (iii) the type of averaging that governs the behavior of geotechnical structures. By assuming that the local average statistics for which the overall behavior of a PVD system is affected can be represented by the geometric average of the actual spatially variable soil (note that the geometric average represents the ‘natural’ average of the lognormal distribution), the relationships between the local average statistics, and ideal point mean, μ_{c_h} , and standard deviation, σ_{c_h} , can be expressed as follows [29]:

$$\mu_{c_h} = \mu_D \exp \left[\ln(1 + v_D^2) \left\{ \frac{1 - \gamma(D)}{2\gamma(D)} \right\} \right] \tag{5}$$

$$\sigma_{c_h} = \sqrt{\left(\mu_{c_h}^2 \left[\exp \left\{ \frac{\ln(1 + v_D^2)}{\gamma(D)} \right\} - 1 \right] \right)} \tag{6}$$

where μ_D and v_D ($v_D = \sigma_D / \mu_D$ in which σ_D is the local average standard deviation of c_h) are, respectively, the local average mean and coefficient of variation of c_h and $\gamma(D)$ is the variance

reduction factor corresponding to the underlying normal random field $\ln(c_h)$, which is a function of the size of the averaging domain and correlation structure of the soil. (Note that by providing appropriate geometric dimensions for the single-drain and multi-drain problems, $\gamma(D)$ for both resolutions can be computed numerically for various $\theta_{\ln c_h}$ from the algorithm presented in Appendix A.)

As the local average statistics depend on the variance reduction factor (i.e., a function of the size of the averaging domain D and correlation length θ or merely a function of the normalized correlation length Θ , which is the ratio of the correlation length to the size of the averaging domain, i.e., $\Theta = \theta/D$), it is possible (Equations (5) and (6)) that the same underlying local average statistics for any two soil domains of different dimensions may be achieved through two approaches, as follows: (i) by employing different correlation lengths, $\theta_{\ln c_h}$, while μ_{c_h} and σ_{c_h} are kept the same through providing the same $\gamma(D)$ and (ii) by employing different μ_{c_h} and σ_{c_h} , while $\theta_{\ln c_h}$ is kept the same through providing different $\gamma(D)$. The first approach is denoted herein as Approach 1 (or A1), while the second approach is denoted as Approach 2 (or A2), and they will be presented in the next sections in more detail. In the following sections, the results of the parametric studies performed to investigate the possible stochastic equivalence of the degree of consolidation between the single-drain and multi-drain analyses for both approaches are compared and discussed in some detail in the succeeding discussion.

Approach 1

The use of different $\theta_{\ln c_h}$ while considering μ_{c_h} and σ_{c_h} as constant parameters is a possible way of obtaining the same underlying local average statistics for soil domains with different dimensions. For the purpose of generalization, a particular domain is often expressed with respect to the normalized form of θ , over the influence zone, D , as utilized by many researchers (e.g., [9, 28, 30–32]). This means that the domain D_1 , employing certain θ_1 , can be considered to be representative of another domain D_2 ($D_2 \neq D_1$) with different θ_2 provided that μ_{c_h} and σ_{c_h} remain the same irrespective of the domain size. The value of θ_2 that needs to be assigned for D_2 can be obtained from the following proposed expression:

$$\frac{\theta_1}{D_1} = \frac{\theta_2}{D_2} = \Theta \quad (7)$$

where Θ is the normalized correlation length, as defined earlier. Following Equation (7), the effect of using θ_1 and θ_2 for D_1 and D_2 (i.e., the same Θ), respectively, will yield the same underlying local average statistics μ_D and σ_D for both domains, subsequently may lead to identical probabilistic results. In other words, if θ_1 and θ_2 follow Equation (7), the point variance will be reduced by the same amount for averaging over D_1 and D_2 (i.e., $\gamma(D_1) = \gamma(D_2)$). For convenience of presentation in the current study, the domain size of single-drain and 16-drain systems are denoted as D_{1d} and D_{16d} , respectively.

Approach 2

Assigning different μ_{c_h} and σ_{c_h} for the single-drain system while keeping $\theta_{\ln c_h}$ as a constant parameter is another way of obtaining the same underlying local average statistics to those of the multi-drain system. Under this approach, μ_{c_h} and σ_{c_h} related to the single-drain system are computed using Equations (5) and (6), by substituting the local average statistics (i.e., μ_D and σ_D) with those obtained from the specified random field parameters of the multi-drain system and $\gamma(D)$ corresponding to the single-drain system (i.e., $\gamma(D_{1d})$). It should be noted that although $\theta_{\ln c_h}$ is the same for both resolutions under this approach, $\gamma(D_{1d}) \neq \gamma(D_{16d})$ as $D_{1d} \neq D_{16d}$. In the sections that follow, Approach 1 and Approach 2 of the single-drain analyses are denoted as SD-A1 and SD-A2, respectively, for convenience of presentation.

In order to investigate the stochastic equivalence between the single-drain and multi-drain solutions under both approaches of obtaining the same underlying local average statistics, a series of FEMC analyses is performed for both the single-drain and multi-drain cases, and the results are compared. The random field parameters for the 16 drain cases and their corresponding single-drain analyses under both approaches are shown in Table I. The 16-drain cases under each specified $\theta_{\ln c_h}$ with constant $\mu_{c_h} = \sigma_{c_h} = 15 \text{ m}^2/\text{year}$ (i.e., $v_{c_h} = 100\%$), as shown in Table I (columns 1–3), are selected for

Table I. Random field parameters assigned to single-drain (both for Approach 1 and Approach 2) analyses for providing the same local average statistics as that of the multi-drain cases.

16 drains in square			Single drain								
			Approach 1			Approach 2					
Point statistics	SOF	Local average statistics (same for both single and 16 drains)	Point statistics (same as 16 drains)	Adjusted SOF	Adjusted point statistics	SOF (same as 16 drains)	SOF				
μ_{c_h} (m ² /year)	σ_{c_h} (m ² /year)	θ_{inc_h} (m)	Θ (θ_{inc_h}/D_{1ed})	μ_D (m ² /year)	σ_D (m ² /year)	$\mu_{c_h}^*$ (m ² /year)	$\sigma_{c_h}^*$ (m ² /year)	μ_{c_h} (m ² /year)	σ_{c_h} (m ² /year)	θ_{inc_h} (m)	
15.0	15.0	0.5	0.1315	10.69	1.355	15.0	15.0	0.125	11.025	3.127	0.5
		1.0	0.263	10.89	2.533			0.25	11.305	4.17	1.0
		4.0	1.05	12.24	7.046			1.0	12.725	8.435	4.0
	($v_{c_h} = 100\%$)	16.0	4.21	13.93	11.853		($v_{c_h} = 100\%$)	4.0	14.171	12.555	16.0
		100.0	26.31	14.8	14.403			25.0	14.85	14.55	100.0
					($v_D = 12.67\%$)				($v_{c_h} = 28.36\%$)		
					($v_D = 23.26\%$)				($v_{c_h} = 36.88\%$)		
					($v_D = 57.56\%$)				($v_{c_h} = 66.28\%$)		
					($v_D = 85.1\%$)				($v_{c_h} = 88.6\%$)		
					($v_D = 97.32\%$)				($v_{c_h} = 97.98\%$)		

the purpose of comparison. The local average statistics for the 16 drain system for each selected θ_{inc_h} are then computed using Equations (5) and (6) and are summarized in Table I (columns 5 and 6). The normalized scale of fluctuation (SOF), Θ , for the 16-drain system is also shown in Table I (column 4). In order to provide the same μ_D and σ_D in case SD-A1, Θ needs to be same as that of its corresponding 16-drain analysis. Accordingly, different θ_{inc_h} are assigned in case SD-A1 (column 9) during the FEMC analysis, calculated based on its corresponding Θ , while μ_{c_h} and σ_{c_h} (columns 7 and 8) remain the same as those of the 16-drain counterpart. On the other hand, μ_{c_h} and σ_{c_h} related to case SD-A2 for providing the same μ_D and σ_D to those of the 16-drain cases are calculated following the procedure discussed earlier and summarized in Table I (columns 10 and 11). In case SD-A2, θ_{inc_h} (column 12) remains the same as that of its corresponding 16-drain analysis. It is clear from Table I that the input variability for the single-drain cases is reduced from that of the 16-drain cases either by employing smaller θ_{inc_h} (in case A1) or by providing lower v_{c_h} (in case A2) to obtain the same μ_D and σ_D to those of the 16-drain system. This is expected because of the fact that the smaller averaging domain for the unit cell analysis would lead to less variance reduction within the influence zone than for the 16-drain domain, which is counterbalanced by assigning smaller θ_{inc_h} or lower v_{c_h} for the unit cell. The results obtained from the 16-drain system and both approaches of the single-drain FEMC analyses employing their corresponding μ_{c_h} , σ_{c_h} , and θ_{inc_h} (as shown in Table I) are compared in terms of μ_U , σ_U , and $P[U \geq U_{90}]$, as depicted in Figures 6–8, in which μ_U , σ_U , and

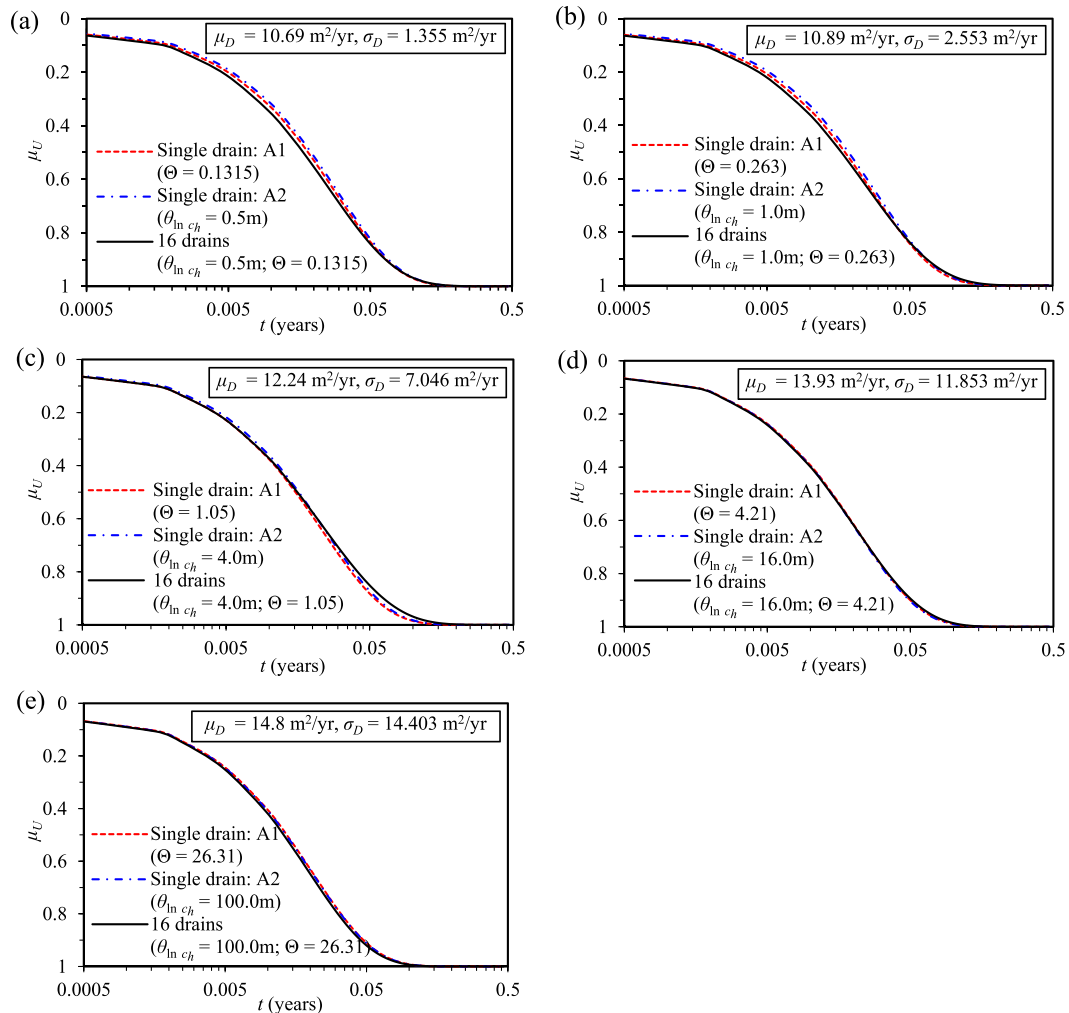


Figure 6. Comparison between single (under Approaches 1 and 2) and multi-drain analyses with respect to μ_U over a range of same local average statistics.

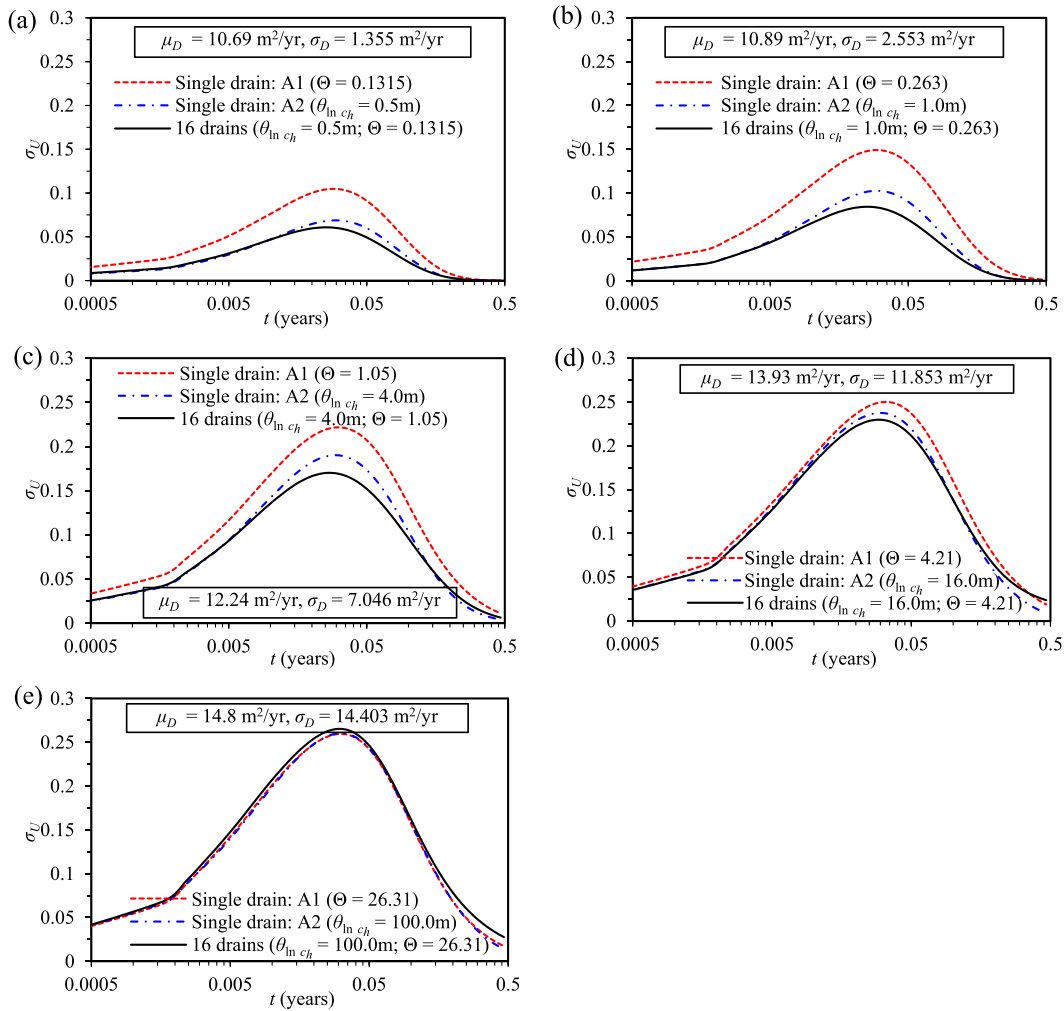


Figure 7. Comparison between single (under Approaches 1 and 2) and multi-drain analyses with respect to σ_U over a range of the same local average statistics.

$P[U \geq U_{90}]$ are expressed as functions of the consolidation time t . It should be noted that the results of case SD-A1 and the 16-drain system are compared with respect to Θ because Θ is same for these two solutions. On the other hand, $\theta_{\ln c_h}$ is the same for case SD-A2 and 16-drain system; therefore, their results are compared based on $\theta_{\ln c_h}$.

The agreement between both approaches of the single-drain and multi-drain solutions in terms of μ_U under various μ_D and σ_D is emphasized in Figure 6, which shows that for a particular correlation length or SOF, μ_U obtained from the single-drain and multi-drain cases are almost identical, implying that both approaches yield equivalent μ_U . The equivalence between the single-drain and multi-drain analyses is further examined via matching the estimated σ_U at different values of local average statistics, as shown in Figure 7. It can be seen that considerable differences in σ_U obtained from case SD-A1 and 16-drain solution are found particularly when Θ is as low as 1.05. When Θ is as low as 0.13 and 1.05, the difference in σ_U between the two solutions is about 73% and 30%, respectively. On the other hand, little or no difference in σ_U (less than 10%) is found when $\Theta \geq 4.21$. This means that the difference in σ_U between case SD-A1 and 16-drain solutions is the smallest for the highest value of Θ and this difference is inversely the highest for the smallest value of Θ . Figure 7 also shows that unlike case SD-A1, case SD-A2 yields very good agreement compared with the multi-drain analyses with respect to σ_U for all cases of $\theta_{\ln c_h}$. It should be noted that the maximum difference in σ_U between case SD-A2 and 16-drain solution at time corresponding to the maximum value of σ_U is 12%, and this is found to correspond to $\theta_{\ln c_h} = 0.5$ m.

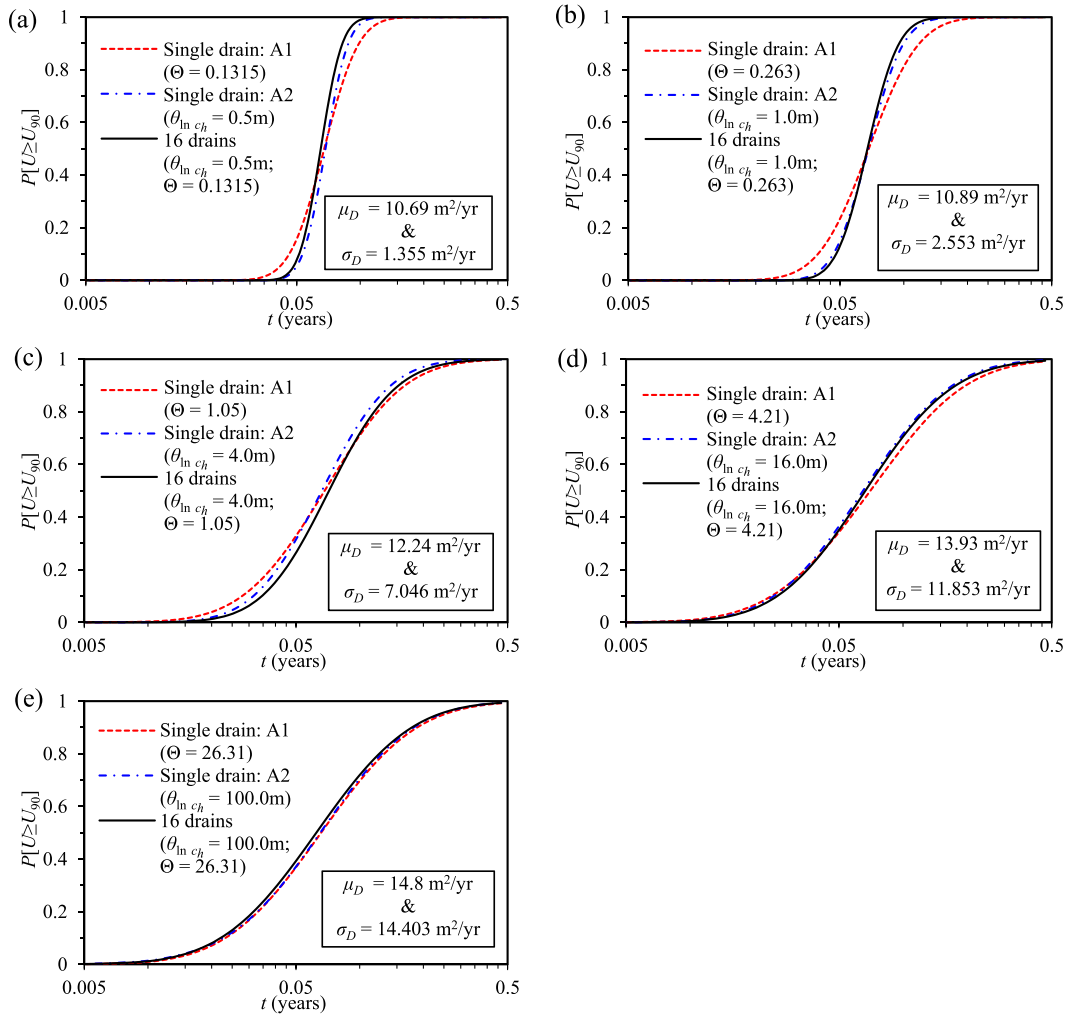


Figure 8. Comparison between single (under Approaches 1 and 2) and multi-drain analyses with respect to $P[U \geq U_{90}]$ over a range of same local average statistics.

Although emerges from the same theoretical background, case SD-A1 produces higher discrepancy in σ_U than case SD-A2 when compared with the multi-drain solution. This discrepancy in σ_U may be attributed to the fact that the decay pattern of the correlation function in the multi-drain system is different from that of case SD-A1 as θ_{inc_h} in each case is different. When $\theta_{inc_h} \leq D$, different random field distributions between the two domains occur, leading to different excess pore water pressure distributions. On the other hand, when $\theta_{inc_h} \geq D$, the decay pattern of the correlation function in case SD-A1 becomes similar to that of the individual drain of the multi-drain system, and thus, the discrepancy in σ_U gradually disappears.

The agreement between the single-drain and multi-drain solutions in terms of $P[U \geq U_{90}]$ under various μ_D and σ_D is illustrated in Figure 8. It can be seen that for any probability level $>50\%$, that is, $P[U \geq U_{90}] > 0.5$ (note that the probability of achieving a target degree of consolidation of interest is greater than 50%), $P[U \geq U_{90}]$ obtained from case SD-A1 is significantly lower (conservative) than its corresponding $P[U \geq U_{90}]$ obtained from the multi-drain system when $\Theta \leq 1.05$. The difference in $P[U \geq U_{90}]$ between the two solutions is insignificant for any $\Theta \geq 4.21$. This is because in this range of Θ , σ_U from case SD-A1 is higher than its multi-drain counterpart, whereas μ_U is identical for each solution strategies. On the other hand, as can be seen from Figure 8, case SD-A2 yields very good agreement with the multi-drain analyses with respect to $P[U \geq U_{90}]$ for all cases of θ_{inc_h} .

From the aforementioned results, it is clear that Approach 1 of the single-drain analysis using the same underlying local average statistics to the multi-drain cases does not seem to produce

reasonable equivalence in terms of the standard deviation of the degree of consolidation and in turn the probability of achieving a target degree of consolidation, except for extremely large correlation length in comparison with the size of the problem domain. However, the good agreement between Approach 2 of the single-drain and multi-drain analyses in terms of μ_U , σ_U , and $P[U \geq U_{90}]$ indicates that the stochastic equivalence between the unit cell analyses and multi-drain solutions can be established by assigning appropriate representative input statistical parameters for the idealized unit cell, which can be computed from the statistical parameters assigned to the multi-drain system, keeping the correlation length the same for both domains in such a way that their underlying local average statistics remain also the same.

Due to the promising results obtained from Approach 2 in establishing the stochastic equivalence between the single-drain and multi-drain systems, Approach 2 is further examined for (i) different random field generation method; (ii) another domain shape of the multi-drain system; and (iii) taking into account the smear effect. The parametric studies performed under each of the aforementioned situations are based on the same local average statistics for both the single-drain and multi-drain resolutions, for each specified θ_{inc_h} , and the associated point statistics of the soil domain of interest are derived using Equations (5) and (6). The mean, μ_D , and coefficient of variation, v_D , of the locally averaged c_h are arbitrarily selected to be equal to 15 m²/year and 0.2, respectively, and the results are presented in Figures 9–11. It should be noted that the results for $\theta_{\text{inc}_h} = 16.0$ m are omitted from Figures 9–11 to enhance the readership of figures. For the same reason, results for smaller θ_{inc_h} (i.e., $\theta_{\text{inc}_h} = 0.5$ and 4.0 m) are presented on the left-hand side, while the results of larger θ_{inc_h} (i.e., $\theta_{\text{inc}_h} = 4.0$ and 100.0 m) are illustrated on the right hand-side in each graph of Figures 9–11.

- *Effect of random field generation method*

As mentioned earlier, the LAS algorithm generates realizations of c_h in the form of grid of cells that are assigned locally averaged values of c_h by taking full account of the FEs size in the local averaging process, which is analogous to that of the large-scale averaging process shown earlier. In this section, the sensitivity of the multi-drain response to the random field discretization method is examined by comparing the results obtained using the LAS method with those obtained employing another random field generation method. Apart from the LAS method, there are several other methods that can be used such as the Karhunen–Loève (K-L) expansion method and the expansion optimal linear estimation (EOLE) method, and in the current study, the K-L expansion method is used. The expression of the lognormal random field of c_h using the K-L expansion method is given by (e.g., [33])

$$c_h(X, \psi) \approx \exp \left[\mu_{\text{inc}_h} + \sum_{i=1}^M \sqrt{\lambda_i} \phi_i(X) \zeta_i(\psi) \right] \tag{8}$$

where X denotes the spatial coordinates, ψ indicates the stochastic nature of the random field, M is the size of the series expansion, λ_i and ϕ_i are the eigenvalues and eigenfunctions of the covariance function, and $\zeta_i(\psi)$ is a vector of standard uncorrelated random variables. The choice of the number of terms M in the K-L expansion method depends on the desired accuracy of the problem at hand. In this paper, this number is taken to be equal to 1000, which corresponds to a maximal error estimate of 18% for the worst situation considered (i.e., $\theta_{\text{inc}_h} = 0.5$ m). The same correlation function given in Equation (1) is used in this case. Details of the K-L expansion method is beyond the scope of this paper and can be found elsewhere (e.g., [34, 35]).

In this part of the parametric study, it is assumed that μ_D and v_D of the locally averaged c_h over the soil domain of interest for each specified θ_{inc_h} are taken to be equal to 15 m²/year and 0.2, respectively. The given local average statistics are then used to derive the associated point statistics for the square area of the 16 drains, which is required for generating the random field of c_h . By substituting the given μ_D , v_D , and computed values of $\gamma(D)$ corresponding to each specified θ_{inc_h} in Equations (5) and (6), μ_{c_h} and σ_{c_h} are calculated for the 16 drains, and the results are summarized in Table II (columns 2 and 3). Using the statistical parameters shown in Table II (columns 1–3), the 16 drains square domain is discretized using both the LAS and K-L expansion methods, and the FEMC analyses are performed. The stochastic response of the 16 drains obtained from the FEMC analyses using both the LAS and K-L expansion random field discretization methods for various θ_{inc_h} is

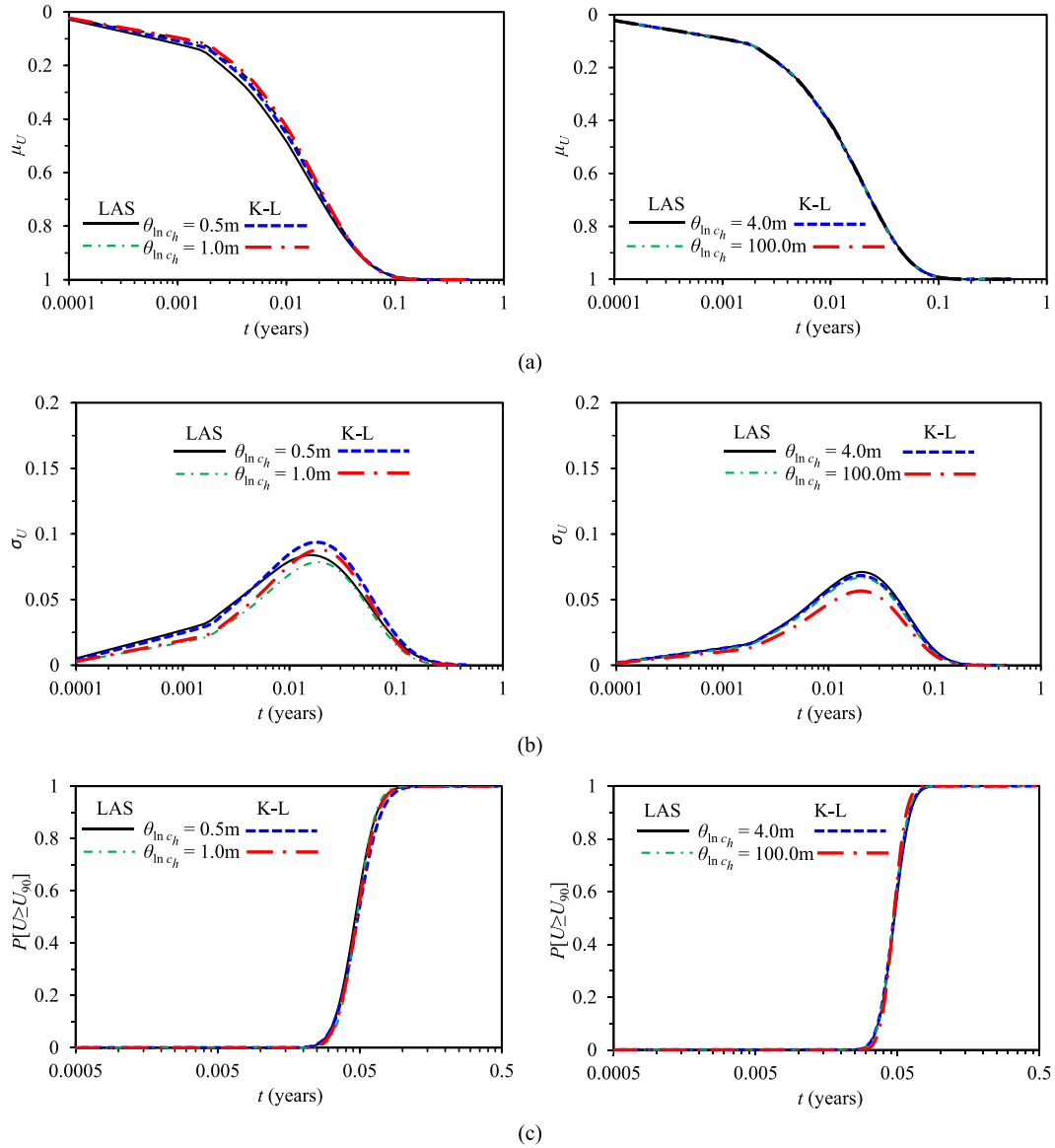


Figure 9. Effect of random field generation method on (a) μ_U , (b) σ_U , and (c) $P[U \geq U_{90}]$ obtained from the multi-drain (16 drains in square domain) analyses for various θ_{inc_h} .

compared in terms of μ_U , σ_U , and $P[U \geq U_{90}]$, and the results are shown in Figure 9. It can be seen that μ_U (Figure 9a), σ_U (Figure 9b), and $P[U \geq U_{90}]$ (Figure 9c) obtained from both random field methods (i.e., LAS and K-L expansion) are nearly identical for a particular θ_{inc_h} . More specifically, the maximum difference in μ_U between the two random field discretization methods is less than 2% throughout the consolidation process for $\theta_{inc_h} = 0.5$ m. On the other hand, a maximal difference of 15% in σ_U is obtained in the case of $\theta_{inc_h} = 100$ m at time corresponding to the peak value of σ_U . However, for any probability level $>50\%$, the maximum difference in $P[U \geq U_{90}]$ is found to be less than 5% for $\theta_{inc_h} = 100$ m. As a conclusion, the probabilistic outputs of the degree of consolidation are insensitive to the random field generation method. Therefore, the LAS method is adopted for random field generation of the remaining FEMC analyses of this study.

• *Effect of domain shape*

So far, the stochastic equivalence between the unit cell and multi-drain solutions is examined over a square domain of multi-drain system. However, in practice, PVD-improved ground may take different

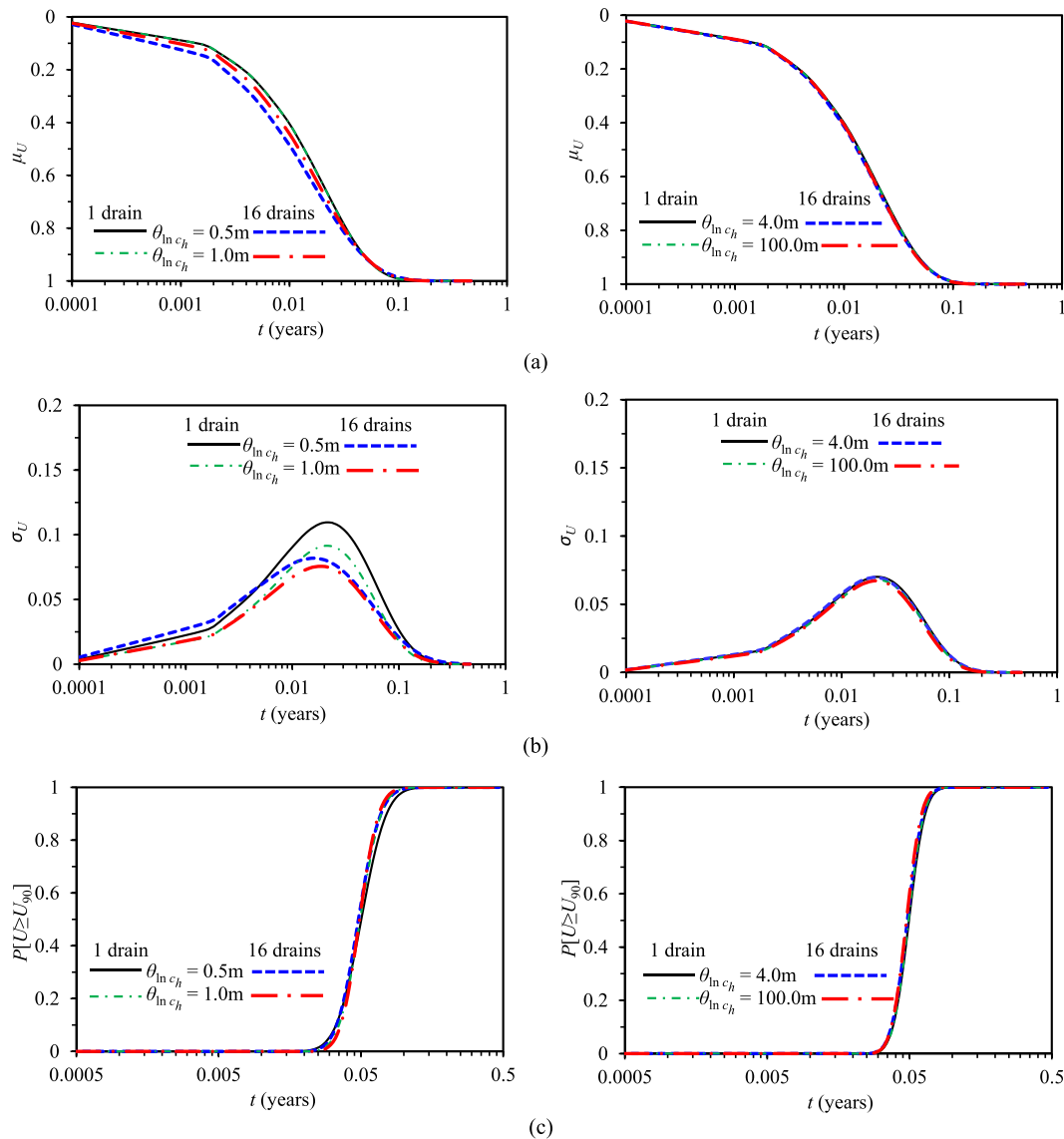


Figure 10. Effect of domain shape on the equivalence of (a) μ_U , (b) σ_U , and (c) $P[U \geq U_{90}]$ obtained from the single-drain and multi-drain analyses (16 drains in rectangular domain) for various θ_{lnc_h} .

shapes other than square. Therefore, the effect of the rectangular domain shape for the multi-drain system on the stochastic equivalence between the single-drain unit cell and multi-drain analyses is examined herein. For this purpose, the 16 drains are assumed to be installed over a rectangular area in two rows with eight drains in each row so that the width to length ratio (i.e., width W in x -direction/length L in y -direction) of the area is 1:4. The representative point statistics (i.e., μ_{c_h} and σ_{c_h}) for both the single-drain and multi-drain (in a rectangular domain) cases are then computed using the given local average statistics (i.e., $\mu_D = 15 \text{ m}^2/\text{year}$ and $v_D = 0.2$) and their respective values of $\gamma(D)$ in Equations (5) and (6), which are summarized in Table II (columns 4–7). The values of μ_{c_h} and σ_{c_h} for the rectangular domain show slightly different values from those of the square domain, and this is because $\gamma(D)$ values for the square domain case are different from those of the rectangular case. The FEMC analyses for both the single-drain and multi-drain for the rectangular domain are performed using their respective values of μ_{c_h} , σ_{c_h} , and θ_{lnc_h} , and the results are shown in Figure 10. It can be seen that, as with the square domain, μ_U (Figure 10a), σ_U (Figure 10b), and $P[U \geq U_{90}]$ (

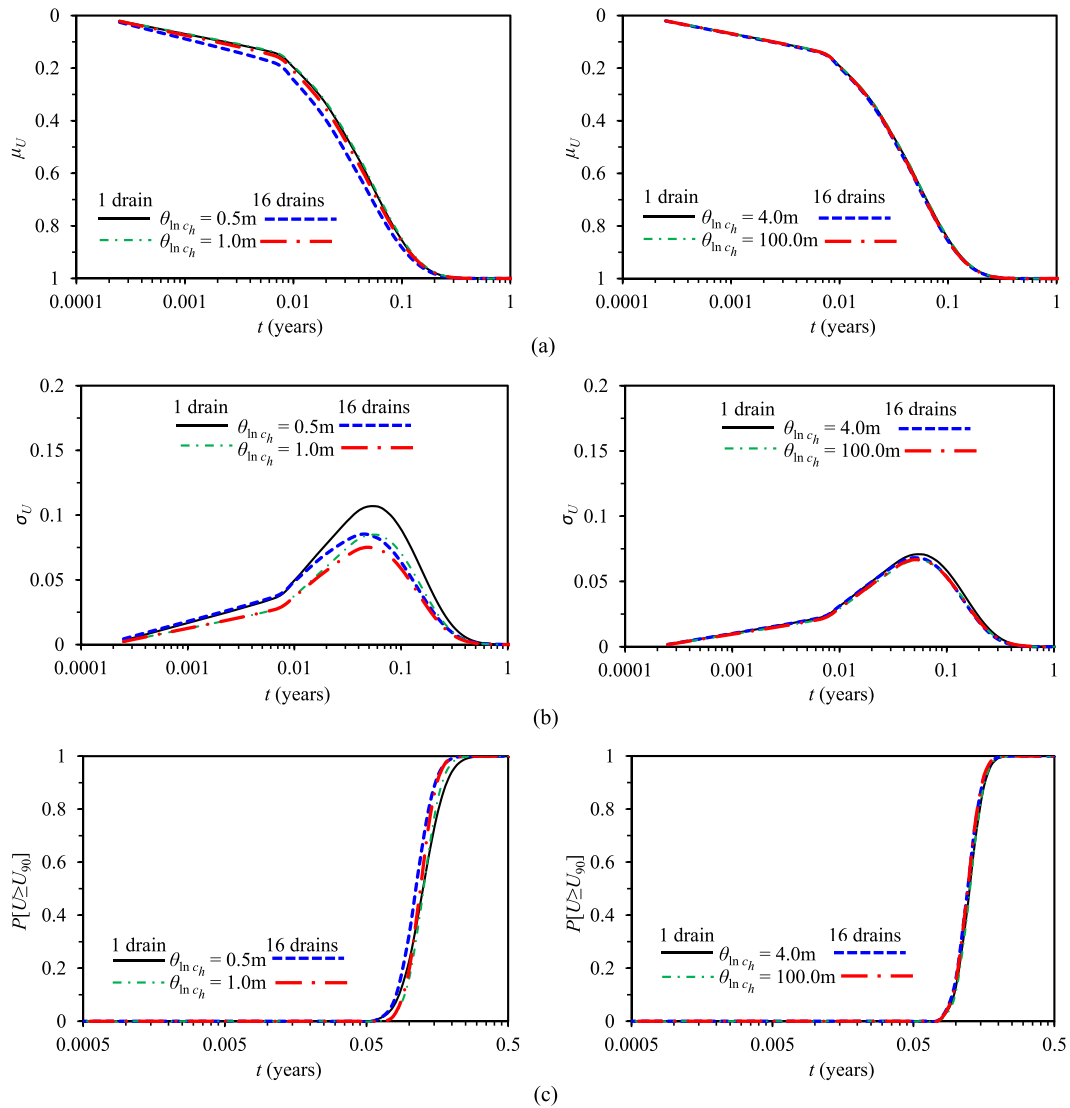


Figure 11. Effect of smear on the equivalence of (a) μ_U , (b) σ_U , and (c) $P[U \geq U_{90}]$ obtained from the single-drain and multi-drain analyses for various θ_{inc_h} .

Table II. Estimated point mean and standard deviation computed from the given local average statistics.

SOF θ_{inc_h}	16 drains in square domain		16 drains in rectangular domain		Single-drain	
	μ_{c_h}	σ_{c_h}	μ_{c_h}	σ_{c_h}	μ_{c_h}	σ_{c_h}
0.5	34.50	73.20	36.27	81.74	16.18	7.41
1.0	19.04	15.65	19.62	17.34	15.40	4.87
4.0	15.42	4.87	15.57	5.40	15.08	3.41
16.0	15.08	3.41	15.11	3.55	15.02	3.10
100.0	15.01	3.06	15.02	3.08	15.003	3.01

Figure 10c) obtained from the FEMC analyses for both the single-drain and multi-drain systems considering rectangular domain are almost identical (the maximal difference in σ_U at time corresponding to the maximum value of σ_U is found to be 19% for $\theta_{\text{inc}_h} = 0.5$ m), implying that the stochastic equivalence is independent of the domain shape.

• *Effect of smear zone*

During mandrel installation of PVDs, a disturbed zone (i.e., smear zone) of reduced permeability is produced. However, soil spatial variability in the smear zone persists [36], albeit the fact that it is no longer fully natural. Although the intensity and extent of smearing depends on factors such as the mandrel size, installation procedure, and soil type [20, 37, 38], it is unavoidable in any PVD soil improvement project. Therefore, it is important to investigate the effect of smear on the stochastic equivalence between the single-drain and multi-drain analyses. The ratio k_h/k'_h (where k_h and k'_h are the horizontal permeability in the undisturbed and smear zones, respectively), which may vary from 2 to 6 as reported by various researchers (e.g., [12, 17]), is assumed to be equal to 3. It can be noticed that no explicit permeability parameter is considered in this study. Accordingly, to simulate such reduced permeability condition in the smear zone during the FE analysis, it is assumed that $k_h/k'_h = c_h/c'_h$ (where c'_h is the horizontal coefficient of consolidation in the smear zone), that is, c_h/c'_h is taken to be equal to 3. The 16 drains in a square area is selected as the multi-drain problem, and it is assumed that the equivalent radius of the smear zone $r_s = 0.197$ m. However, a square shaped of a smear zone of side length $S_s = 0.35$ m ($S_s = \sqrt{\pi r_s^2}$) is modeled at the center of each individual drain to avoid the unfavorable mesh shape for the LAS method.

At this point, it is worthwhile mentioning that in geotechnical engineering, the random field models are often non-stationary in their mean; however, the variance and covariance structure are generally assumed to be stationary because they need prohibitive volumes of data to estimate their parameters [29]. Accordingly, the variance and covariance structure of c_h are assumed to be stationary, while a non-stationary mean is used to take into account the smear effect. This means that c_h varies spatially in such a way that its second moment structures (variance, covariance, and so on) in the undisturbed and smear zones are identical with respect to the mean, that is, $v_{c_h} = v_{c'_h}$, $\theta_{\text{In}c_h} = \theta_{\text{In}c'_h}$ (where $v_{c'_h}$ and $\theta_{\text{In}c'_h}$ are, respectively, the coefficient of variation and correlation length of the smear zone). Under this argument, the mean, μ'_D , and coefficient of variation, v'_D , of the local average measurement of c_h in the smear zone are assumed to be equal to 5 and $0.2 \text{ m}^2/\text{year}$, respectively. By substituting the given μ'_D , v'_D , and respective $\gamma(D)$ corresponding to a particular $\theta_{\text{In}c_h}$ in Equations (5) and (6), the point mean, $\mu_{c'_h}$, and standard deviation, $\sigma_{c'_h}$, of the smear zone are computed for both the single-drain and multi-drain analyses for various $\theta_{\text{In}c_h}$, as summarized in Table III.

In order to simulate the smear effect during the FE analysis of the multi-drain system, two independent random fields of c_h are generated. By making use of the specified μ_{c_h} and σ_{c_h} (Table II) into the LAS method, a random field of c_h is generated first for the whole soil domain and mapped onto the corresponding grid of the FE mesh. Then another random field of c_h is generated using the same seed number of the previously generated field (for the whole soil domain of interest) with $\mu_{c'_h}$ and $\sigma_{c'_h}$ (Table III). However, for both random fields, the same value of $\theta_{\text{In}c_h}$ is used. Now from the second random field, only the corresponding elements to the smear zone are mapped onto the FEs mesh. The same random field generation process is also followed for the FE analysis of the single-drain counterpart. This process of random field generation ensures the original random nature of c_h over the soil domain and reasonably reflects the smear effect as well.

Table III. Estimated point mean and standard deviation in the smear zone computed from the given local average statistics.

SOF $\theta_{\text{In}c'_h}$	Single drain		16 drains in square domain	
	$\mu_{c'_h}$	$\sigma_{c'_h}$	$\mu_{c'_h}$	$\sigma_{c'_h}$
0.5	5.39	2.47	11.5	24.4
1.0	5.14	1.62	6.346	5.215
4.0	5.026	1.137	5.14	1.62
16.0	5.006	1.033	5.026	1.137
100.0	5.001	1.005	5.004	1.02

Following the aforementioned random field generation process, the FEMC analyses corresponding to various θ_{inc_h} are performed for both the single-drain and multi-drain systems, and the equivalence between the two solutions in terms of μ_U , σ_U , and $P[U \geq U_{90}]$ are examined, and their results are depicted in Figure 11. It can be seen that, as with the case of no smear, μ_U (Figure 11a), σ_U (Figure 11b), and $P[U \geq U_{90}]$ (Figure 11c) obtained from the single-drain analysis agree well with those obtained from the multi-drain analysis, for all cases of θ_{inc_h} .

The overall results presented in this section indicate that the behavior of PVD-improved ground is governed by the local average soil properties instead of the point soil properties. The results also demonstrate that the geometric average, which is lying between the arithmetic and harmonic averages, is a reasonable approach to estimating the local average soil properties for different domain shape even if the smear effect is to be considered.

CONCLUSIONS

This paper used the random field theory and FEs modeling to investigate the stochastic equivalence between the single-drain 'unit cell' and multi-drain solutions for ground improvement by PVDs. The horizontal coefficient of consolidation, c_h , was treated as the most significant random field affecting PVD-improved ground, and an uncoupled 2D FEs soil consolidation analysis was applied.

In the first part of the paper, the point input statistical parameters were assumed to be the same for both the single-drain and multi-drain cases. Despite the reasonable agreement obtained in terms of the mean degree of consolidation, μ_U , for the single-drain and multi-drain analyses irrespective of the input parameters, a significant difference in the standard deviation, σ_U , between the two solutions was found except for extremely large correlation lengths. Therefore, it can be concluded that the point soil properties, which are considered to be representative of a certain domain (over which they are measured), need to be adjusted prior to applying to another domain of different size. This conclusion demonstrates the potential pitfall of using typical statistical soil properties without referencing to the site investigation scale.

In the second part of the paper, it was argued that the stochastic equivalence between the idealized unit cell and multi-drain analyses can be achieved if the local average statistics for both resolutions are the same. Under this reasoning, two groups of stochastic FEMC analyses were performed. In the first group, the same underlying local average statistics for both domains were obtained by employing the same point mean and standard deviation but using different correlation lengths calculated based on the size of the domain. It was found that μ_U obtained from the single-drain analysis agrees very well with that obtained from the multi-drain counterpart. However, considerable discrepancies in σ_U and $P[U \geq U_{90}]$ derived from the two solutions were found except for very high correlation lengths. Therefore, it can be concluded that the method of obtaining the same local average statistics for soil domains with different dimensions by altering the correlation length while keeping the point mean and standard deviation the same is not a reasonable approach to establish stochastic equivalence between the single-drain and multi-drain solutions of PVD-improved ground. In the second group, the same local average statistics for both the single-drain and multi-drain domains were obtained by employing different point mean and standard deviation, while keeping the correlation length the same for both resolutions. Under this method, it was found that μ_U , σ_U , and $P[U \geq U_{90}]$ obtained from the single-drain analysis agree very well with those obtained from the multi-drain analysis, for all selected correlation lengths using different random field generation methods and different domain shapes and considering the smear effect. Therefore, it was concluded that it is not the point statistics soil properties that should be the same for the unit cell but rather the local average soil properties. It was also concluded that the geometric average is a reasonable approach for estimating the local average soil properties for different domain of shapes including the smear effect.

Overall, it was shown that the stochastic equivalence between the unit cell and multi-drain solutions can be established by assigning appropriate representative point statistics for the idealized unit cell, which can be computed from the statistical parameters assigned to the multi-drain by keeping the same correlation length for both domains and using appropriate transformation functions in such a

way that their underlying local average statistics remain the same. The procedure of doing so can be briefly explained as follows: one should first compute the local average statistics for the multi-drain system based on its size and the point statistics of the random field. Then, the same local average statistics as obtained from the multi-drain system need to be adopted for the unit cell to deduce the corresponding point statistics of the unit cell using Equations (5) and (6) of this study.

Although inherent soil variability is essentially 3D, it is limited to 2D random field in the current study. That is, soil is assumed to be spatially variable in the horizontal plane, while soil variability in the vertical direction is ignored. This is because to achieve mathematical convenience as the stochastic solution of 3D variability is very complex and computationally too intensive, particularly for the multi-drain system. Considering 3D soil variability is beyond the scope this paper and will be investigated in future development of the current work.

APPENDIX A. Determination of Variance Reduction Factor

The amount by which the variance is reduced from the point variance as a result of the local averaging can be estimated from the corresponding variance function of the 2D Markov correlation function shown in Equation (1), as follows [29]:

$$\gamma(D) = \gamma(X, Y) = \frac{1}{X^2 Y^2} \times \int_0^X \int_0^X \int_0^Y \int_0^Y \rho(\zeta_1 - \eta_1, \zeta_2 - \eta_2) d\zeta_1 d\eta_1 d\zeta_2 d\eta_2 \tag{A.1}$$

where X and Y are the dimensions of the averaging domain, D , in the x -direction and y -direction, respectively (i.e., $D=X \times Y$). The fourfold integration in Equation (A.1) can be condensed to twofold integration by taking advantage of the quadrant symmetry ($\rho(\tau_1, \tau_2) = \rho(-\tau_1, \tau_2) = \rho(\tau_1, -\tau_2) = \rho(-\tau_1, -\tau_2)$) of the correlation function in Equation (1) and can be expressed as

$$\gamma(X, Y) = \frac{4}{X^2 Y^2} \times \int_0^X \int_0^Y (X - \tau_1)(Y - \tau_2) \rho(\tau_1, \tau_2) d\tau_1 d\tau_2 \tag{A.2}$$

Equation (A.2) can be computed numerically with reasonable accuracy using the 16-point Gaussian quadrature integration scheme, as follows:

$$\gamma(X, Y) = \frac{1}{4} \sum_{i=1}^{16} \omega_i (1 - \vartheta_i) \sum_{j=1}^{16} \omega_j (1 - \vartheta_j) \rho(\zeta_i, \eta_j) \tag{A.3}$$

$$\zeta_i = \frac{X}{2} (1 + \vartheta_i), \eta_j = \frac{Y}{2} (1 + \vartheta_j) \tag{A.4}$$

where ω_i and ϑ_i are the weights and Gauss points, respectively.

REFERENCES

1. Rowe PW. The relevance of soil fabric to site investigation practice. *Geotechnique* 1972; **22**(2):195–300.
2. Bari MW, Shahin MA, Nikraz HR. Probabilistic analysis of soil consolidation via prefabricated vertical drains. *International Journal of Geomechanics (ASCE)* 2013; **13**(6):877–881.
3. Bari MW, Shahin MA, Nikraz HR. Effects of soil spatial variability on axisymmetric versus plane strain analyses of ground improvement by prefabricated vertical drains. *International Journal of Geotechnical Engineering* 2012; **6**(2):139–147.
4. Hong HP, Shang JQ. Probabilistic analysis of consolidation with prefabricated vertical drains for soil improvement. *Canadian Geotechnical Journal* 1998; **35**(4):666–677.
5. Zhou W, Hong HP, Shang JQ. Probabilistic design method of prefabricated vertical drains for soil improvement. *Journal of Geotechnical and Geoenvironmental Engineering* 1999; **125**(8):659–664.
6. Bari MW, Shahin MA. Probabilistic design of ground improvement by vertical drains for soil of spatially variable coefficient of consolidation. *Geotextiles and Geomembranes* 2014; **42**(1):1–14.

7. Indraratna B, Redana IW. Numerical modeling of vertical drains with smear and well resistance installed in soft clay. *Canadian Geotechnical Journal* 2000; **37**(1):132–145.
8. Fenton GA, Griffiths DV. Three-dimensional probabilistic foundation settlement. *Journal of Geotechnical and Geoenvironmental Engineering* 2005; **131**(2):232–239.
9. Huang J, Griffiths DV, Fenton GA. Probabilistic analysis of coupled soil consolidation. *Journal of Geotechnical and Geoenvironmental Engineering* 2010; **136**(3):417–430.
10. Fenton GA, Vanmarcke EH. Simulation of random fields via local average subdivision. *Journal of Engineering Mechanics* 1990; **116**(8):1733–1749.
11. Vanmarcke EH. *Random Fields: Analysis and Synthesis*. The MIT Press: Massachusetts, 1984.
12. Hansbo S. Consolidation of fine-grained soils by prefabricated drains. *Proceedings of the 10th International Conference on Soil Mechanics and Foundation Engineering*. Stockholm, Sweden, 1981;677–682.
13. Chang CS. Uncertainty of one-dimensional consolidation analysis. *Journal of Geotechnical Engineering* 1985; **111**(12):1411–1424.
14. Fournier A, Fussell D, Carpenter L. Computer rendering of stochastic models. *Communications of the ACM* 1982; **25**(6):371–384.
15. Fenton GA. *Simulation and Analysis of Random Fields, in Department of Civil Engineering and Operations Research*. Princeton University: New Jersey, 1990.
16. Smith IM, Griffiths DV. *Programming the Finite Element Method* (4th). John Wiley and Sons: Chichester, West Sussex, 2004.
17. Chu J, Bo MW, Choa V. Practical considerations for using vertical drains in soil improvement projects. *Geotextiles and Geomembranes* 2004; **22**(1–2):101–117.
18. Ching J, Phoon K-K. Effect of element sizes in random field finite element simulations of soil shear strength. *Computers & Structures* 2013; **126**(1):120–134.
19. Harada T, Shinozuka M. The scale of correlation for stochastic fields – technical report. Department of Civil Engineering and Engineering Mechanics, Columbia University: New York, 1986.
20. Bo MW, Chu J, Low BK, Choa V. *Soil Improvement: Prefabricated Vertical Drain Techniques*. Thomson Learning: Singapore, 2003.
21. Beacher GB, Christian JT. *Reliability and Statistics in Geotechnical Engineering*. John Wiley & Sons: Chichester, England, 2003.
22. Phoon K-K, Kulhawy FH. Characterization of geotechnical variability. *Canadian Geotechnical Journal* 1999; **36**(4):612–624.
23. Popescu R, Deodatis G, Prevost JH. Bearing capacity of heterogeneous soils – a probabilistic approach. *Proceedings of the 55th Canadian Geotechnical and 3rd Joint LAH-CNC and CGS Ground Water Specialty Conference*. Niagara falls, Ontario, 2002;1021–1027.
24. Fenton GA. Estimation for stochastic soil models. *Journal of Geotechnical and Geoenvironmental Engineering* 1999; **125**(6):470–485.
25. Gong W, Luo Z, Juang CH, Huang H, Zhang J, Wang L. Optimization of site exploration program for improved prediction of tunneling-induced ground settlement in clays. *Computers and Geotechnics* 2014; **56**:69–79.
26. Vanmarcke EH. Probabilistic modelling of soil profiles. *Journal of Geotechnical Engineering Division* 1977; **103**(11):1227–1246.
27. Fenton GA, Griffiths DV, Cavers W. Resistance factors for settlement design. *Canadian Geotechnical Journal* 2005; **42**(5):1422–1436.
28. Fenton GA, Griffiths DV. Bearing-capacity prediction of spatially random c - ϕ soils. *Canadian Geotechnical Journal* 2003; **40**(1):54–65.
29. Fenton GA, Griffiths DV. *Risk Assessment in Geotechnical Engineering*. Wiley: New York, 2008.
30. Fenton GA, Griffiths DV, Williams MB. Reliability of traditional retaining wall design. *Geotechnique* 2005; **55**(1):55–62.
31. Griffiths DV, Fenton GA. Probabilistic slope stability analysis by finite elements. *Journal of Geotechnical and Geoenvironmental Engineering* 2004; **130**(5):507–518.
32. Haldar S, Sivakumar Babu GL. Effect of soil spatial variability on the response of laterally loaded pile in undrained clay. *Computers and Geotechnics* 2008; **35**(4):537–547.
33. Cho SE, Park HC. Effect of spatial variability of cross-correlated soil properties on bearing capacity of strip footing. *International Journal for Numerical and Analytical Methods in Geomechanics* 2010; **34**:1–25.
34. Ghanem R, Spanos PD. *Stochastic Finite Elements – A Spectral Approach*. Springer: New York, 1991.
35. Spanos PD, Ghanem R. Stochastic finite element expansion for random media. *Journal of Engineering Mechanics (ASCE)* 1989; **115**(5):1035–1053.
36. Sharma JS, Xiao D. Characterization of a smear zone around vertical drains by large-scale laboratory tests. *Canadian Geotechnical Journal* 2000; **37**(6):1265–1271.
37. Eriksson U, Hansbo S, Torstensson BA. Soil improvement at Stockholm-Arlanda Airport. *Ground Improvement* 2000; **4**(2):73–80.
38. Lo D. Vertical drain performance: myths and facts. *Transactions, Hong Kong Institute of Engineering* 1998; **5**(1):34–50.